Watching the Solvation of Atoms in Liquids One Solvent Molecule at a Time

Arthur E. Bragg, William J. Glover,* and Benjamin J. Schwartz[†]

Department of Chemistry & Biochemistry, University of California, Los Angeles, Los Angeles, California 90095-1569, USA
(Received 9 April 2010; published 11 June 2010)

We use mixed quantum-classical molecular dynamics simulations and ultrafast transient hole-burning spectroscopy to build a molecular-level picture of the motions of solvent molecules around Na atoms in liquid tetrahydrofuran. We find that even at room temperature, the solvation of Na atoms occurs in discrete steps, with the number of solvent molecules nearest the atom changing one at a time. This explains why the rate of solvent relaxation differs for different initial nonequilibrium states, and reveals how the solvent helps determine the identity of atomic species in liquids.

An outstanding question in the physics of liquids is how the motions of solvent molecules affect the electronic structure of dissolved solutes [1]. Is it correct to think of liquids as a continuum, or are the dynamics of individual solvent molecules important? In this Letter, we build a molecular-level picture of the solvent motions around sodium atoms in a solution of liquid tetrahydrofuran (THF) using a synergistic combination of ultrafast spectroscopy and quantum molecular dynamics simulations. Our simulations reveal a correlation between the spectrum of the sodium atom and specific local solvent-solute configurations, and we explore this correlation experimentally using transient hole-burning (THB) spectroscopy. We use the combination of experiments and simulations to decipher the experimentally measured, spectrally resolved nonequilibrium relaxation of Na atoms in solution and thus determine the principle steps in solvation at the molecular level. Even though the transformations we study occur in solution at room temperature, we are able to ''watch'' the solvent molecules rearrange around the relaxing sodium atoms one at a time, a process that we find occurs via discrete rather than continuous changes in the atom's electronic structure in solution.

Our choice to study the solvation of atoms is based on their lack of internal nuclear degrees of freedom, so that the spectral relaxation dynamics of atoms directly reflect the motions of the surrounding solvent and is unobscured by competing intramolecular processes. Our particular choice to examine atomic sodium in liquid THF is based on its electronic structure, which intimately links its absorption spectrum with the local solvent environment. Rather than being an atom that interacts only weakly with the solvent, experiments have suggested that an equilibrated neutral sodium atom in liquid THF is better described as a (Na^+, e^-) tight-contact pair (TCP), a species in which the sodium atom's valence electron is not only partly bound by the sodium nucleus but also extends significantly into the solvent [2,3]. As a result, the spectrum of the neutral sodium TCP in liquid THF peaks at 870 nm (Fig. 1, blue circles [4]), between that of an unsolvated gas-phase sodium atom (which absorbs at 590 nm) and a

THF-solvated electron—i.e., a fully separated Na^+-e^- pair in solution (with absorption peaking at 2100 nm [5]).

To better understand the nature of the neutral sodium TCP in liquid THF and how its absorption spectrum reflects the nature of the local solvent configuration, we performed mixed quantum-classical molecular dynamics (MQC MD) simulations of this system at equilibrium [6] (for details, see the supplementary material [7]). Figure 1(b) features a snapshot of this solute and its first solvent shell from our MQC MD simulations: at equilibrium, we find that the valence electron density (white surface) shifts away from the Na^+ core [blue (dark)
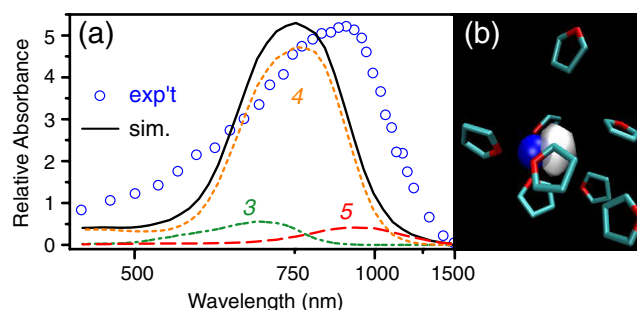

FIG. 1 (color online). (a) Absorption spectrum of the (Na^+, e^-) TCP in room-temperature THF: experimentally measured, blue circles [4]; calculated from our MQC MD simulations, black solid curve. We note that our inhomogeneously broadened simulated spectrum appears narrower than that measured experimentally, suggesting that the simulation does not capture the relative population of coordination motifs precisely; see the supplementary material for details [7]. (b) A snapshot of the (Na^+, e^-) TCP in THF and its first solvent shell from our MQC MD simulations. THF molecules are represented by pentagons, Na^+ with a blue (dark) sphere, and the electron as a white isosurface at 50% of the charge density maximum. The equilibrium TCP is dominated by configurations in which oxygen sites on four local THF molecules (red or dark vertices) coordinate to Na^+. Although this motif contributes heavily to the simulated absorption spectrum [orange short-dashed curve in (a)], fivefold (red dashed curves) and threefold (green dot-dashed curves) motifs also contribute to the full inhomogeneously broadened line shape.

sphere], so that the TCP has a substantial dipole moment (7.2 D on average). Strong attractive interactions between the Na^+ core and oxygen sites on nearby THF molecules provide the driving force for this displacement of the electron density: although pushing the electron density away from the cation core costs energy in the form of partially ionizing the sodium atom, the solvation energy gained from the interaction between the solvent oxygen sites and the partially exposed Na^+ core compensates the charge separation. Our simulations suggest that the optimal balance between cation-solvent interaction and electron displacement is struck when the oxygen sites on four local THF molecules "coordinate" with the Na^+ end of the TCP—what we subsequently refer to as the fourfold-coordinated configuration of this solute-solvent system. Although this configuration dominates at equilibrium, our simulations show that thermal fluctuations also populate threefold-, fivefold-, and, to a lesser extent, twofold-coordinated configurations.

Our MD simulations also reveal that the peak in the absorption spectrum shifts to the red (through visible and to near IR wavelengths) as the number of THF molecules coordinating the cation side of the neutral Na TCP increases [Fig. 1(a)]. This occurs because increased solvent coordination of the cation pushes the electron further from the Na^+ core and reduces valent interactions between the Na^+-e^- pair; thus, the character of a highly coordinated TCP becomes more like a solvated electron and less like a (centrosymmetric) gas-phase sodium atom. Conversely, solvent-solute configurations with fewer than four cation-coordinating solvent molecules allow the electron to interact more strongly with the sodium nucleus, inducing the absorption spectrum to shift to the blue. The fact that multiple cation coordination states exist at equilibrium means that the absorption spectrum of the TCP is inhomogeneously broadened, as shown in Fig. 1(a). Thus, if the solvent motions around an atomic sodium TCP in liquid THF either increase or decrease coordination to the cation end of the TCP, it should be possible to monitor these configurational changes spectroscopically.

To this end, we have used ultrafast THB spectroscopy [8] to interrogate the spectral dynamics that accompany the fluctuations between the different TCP coordination states at equilibrium. Because (Na^+, e^-) is a metastable species that exists in solution only on sub-μs time scales [4], we had to prepare this species for study *in situ* starting from sodium iodide. The relatively strong ion-pairing interactions between Na^+ and I^- ions in liquid THF allow more than 90% of the electrons photodetached from I^- to be captured by the nearby Na^+ cations to create equilibrated (Na^+, e^-) TCPs within a few hundred ps [9,10]. Thus, our THB experiments consist of a sequence of three ultrashort laser pulses [7]. The first pulse at 266 nm photoinitiates electron transfer from I^- to Na^+ to create (Na^+, e^-) TCPs. The second pulse at 800 nm arrives ~0.5 ns later to photoexcite a subensemble of equilibrated TCPs with particular cation coordination numbers, reducing the total number of

absorbing TCP solutes and leaving a transient depletion, or bleach, of the TCP spectrum. The ensemble of TCPs that remain contains the same types of solvent-solute motifs that exist at equilibrium, but at proportions that were not present statistically prior to the sample's interaction with this pulse. Consequently, the same thermally activated fluctuations that cause cation-solvent coordination numbers to change at equilibrium also cause the nonequilibrium ensemble of ground-state TCPs to recover to the equilibrated distribution. Since the TCP's absorption spectrum is inhomogeneously broadened, we use a third, broadband pulse that arrives at a variable time delay to track these fluctuations directly from the spectral evolution of the transient bleach [7].

When we perform this three-pulse experiment, we find that photoexcitation of the equilibrated (Na^+, e^-) TCPs leads to charge separation: excitation moves the TCP valence electron away from the Na^+ out into the liquid. Our data, which are described in detail in the supplementary material [7], show that roughly 90% of the separated electrons remain close enough to their geminate Na^+ cations to recombine rapidly, in ~1 ps, regenerating the parent TCPs. The remaining ~10% of electrons are ejected further out into solution, where they recombine only on a diffusive time scale of hundreds of ps. Once the ~1-ps recombination is complete, it is the long-lived depletion in TCP population that is responsible for the spectral hole left behind following the selective excitation, enabling us to track the dynamics that lead to recovery of the equilibrium distribution [7].

Figure 2(a) shows the THB dynamics that follow 800-nm photoexcitation of (Na^+, e^-) TCPs in liquid THF [7]. The induced absorption appearing above 1200 nm at the earliest time delays originates from the electrons that recombine with nearby Na^+ on a time scale faster than that of the THB dynamics (see the supplementary material [7] for details on electron recombination dynamics). The THB data below 1200 nm reveal two bands with positive intensity centered at 570 and 700 nm and a band with negative intensity centered at 1000 nm. The 570-nm band decays with a ~4-ps lifetime, while the 700-nm feature decays and the 1000-nm bleach recovers on a ~8-ps time scale. The symbols in Fig. 2(c) plot the time dependence of each of these features, determined by integrating the shaded regions shown in Fig. 2(a). The spectral dynamics clearly reflect a two-step kinetic process, with the decay at 570 nm feeding the intensity of the 700-nm feature, whose decay feeds a concomitant recovery at 1000 nm.

Because the solute is an atom, these spectral features can only correspond to differences in local solvent configuration [7]. Thus, guided by the results of our MD simulations [6], we conclude that these spectral features can be assigned to the absorption of (Na^+, e^-) TCPs with different degrees of coordination between Na^+ and oxygen sites on nearby THF molecules. In particular, the 700-nm and 570-nm bands closely match the simulated absorption spectra of TCPs characterized by threefold and twofold
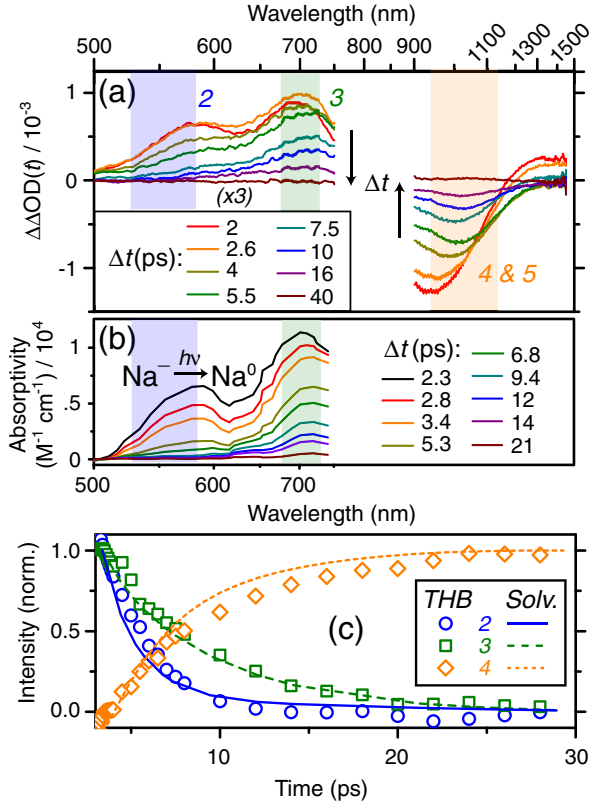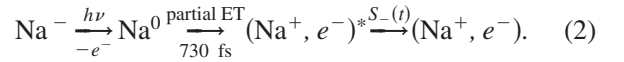
FIG. 2 (color online). (a) Transient hole-burning dynamics of the (Na^+, e^-) TCP following 800-nm excitation [7]. (b) Transient difference spectra for the dynamics that accompany the nonequilibrium relaxation of $(\mathrm{Na}^+, e^-)^*$ created via photodetachment of Na^- in liquid THF $[S_-(t)$ in Eq. (2)] [2,10]. (c) Time dependence of the spectral features in (a) (symbols) and (b) (curves), determined by integrating over the shaded regions. The amplitudes of the transients obtained from the 570- and 700-nm features (representing twofold- and threefold-coordinated TCPs, respectively) are normalized at 4 ps—a time at which the initial recombination kinetics of the nonequilibrated ensemble is complete [7]; the recovery of the 1000-nm band (fourfold- and fivefold-coordinated TCPs) is similarly normalized. The orange dotted curve was derived from the 1130-nm spectral dynamics following photoexcitation of Na^- [2], corresponding to the appearance of higher-coordinated solvent-solute motifs after detachment. Both the THB and nonequilibrium solvation dynamics are dominated by a two-step kinetic process that increases the solvent coordination of the solute: $2 \rightarrow 3 \rightarrow 4$.

cation-solvent coordination, respectively. The simulations also indicate that the dominant fourfold-coordinated solute absorbs near the peak of the equilibrium spectrum, allowing us to assign the bleach centered at 1000 nm as arising primarily from this solvent-solute configuration. The spectral dynamics in Fig. 2(a) and the kinetic traces in Fig. 2(c) thus reflect thermal fluctuations between sets of solvent-solute configurations that differ by the number of coordinating solvent molecules that are arranged with respect to the solute in a specific way:

$$2 \xrightarrow{4 \text{ ps}} 3 \xrightarrow{8 \text{ ps}} 4. \tag{1}$$

Our overall interpretation of the data in Figs. 2(a) and 2(c) can be summarized as follows. Our 800-nm excitation pulse produces a net reduction in the population of sodium TCPs with higher degrees of solvent-cation interaction, which are the TCPs that absorb primarily near 1000 nm. The nonequilibrium ensemble of solvent-solute configurations that remain following excitation is therefore enriched in twofold- and threefold-coordinated TCPs that absorb at 570 and 700 nm. Recovery of the equilibrated ensemble requires a net increase in the degree of solvent-cation coordination; this reconfiguration of local solvent molecules converts the excess twofold- and threefold-coordinated motifs into the missing fourfold- (and fivefold-) coordinated configurations. The overall population of fivefold-coordinated structures is small (Fig. 1), so that the recovery of the fourfold-coordinated TCP dominates the observed bleach spectral dynamics. Thus, we have directly observed the locally coordinated solvent molecules reconfiguring about the atomic solute with a single-solvent-molecule resolution in a room-temperature liquid.

The THB data in Fig. 2(a) provide a direct correlation between the (Na^+, e^-) TCP spectrum and specific solvent-solute configurations that we can use to build a molecular-level picture of the nonequilibrium solvation dynamics that follow the initial creation of this species. We [2] and others [11] previously examined the nonequilibrium solvation of neutral Na TCPs created via electron photodetachment of Na^- in liquid THF. The formation and relaxation of neutral Na created this way proceeds as follows [2,10]:

$$\mathrm{Na}^- \xrightarrow[-e^-]{h\nu} \mathrm{Na}^0 \xrightarrow[730 \text{ fs}]{\text{partial ET}} (\mathrm{Na}^+, e^-)^* \xrightarrow{S_-(t)} (\mathrm{Na}^+, e^-). \tag{2}$$

Because the solvent cavity that accommodates the parent Na^- anion is much larger than the neutral TCP, the nascent Na^0 is "gas-phase-like," with little coordination by the surrounding solvent. Solvent relaxation around the smaller neutral Na atom subsequently induces a partial electron-transfer reaction, creating a nonequilibrated TCP, $(\mathrm{Na}^+, e^-)^*$. The spectrum of the undercoordinated $(\mathrm{Na}^+, e^-)^*$ then shifts further to the red as the local solvent molecules continue to rearrange [designated by the process $S_-(t)$ in Eq. (2)], pushing the electron density off the Na^+ core and bringing the TCP to equilibrium.

Figure 2(b) presents the spectral dynamics that accompany the (nonequilibrium) TCP solvation following e^- photodetachment from Na^-; to better compare this relaxation to the THB data in Fig. 2(a), we have subtracted the equilibrated TCP spectrum (Fig. 1) from the transient spectrum at each time delay [2,10]. Remarkably, the spectral progression plotted in Fig. 2(b) proceeds exactly as we observed in the THB data plotted in Fig. 2(a), with well-defined features at 570 and 700 nm and the former decaying roughly twice as quickly as the latter. The similarity between the photodetachment and THB data indicates that nonequilibrium solvation of the sodium TCP occurs through the same steps and on the same time scales that
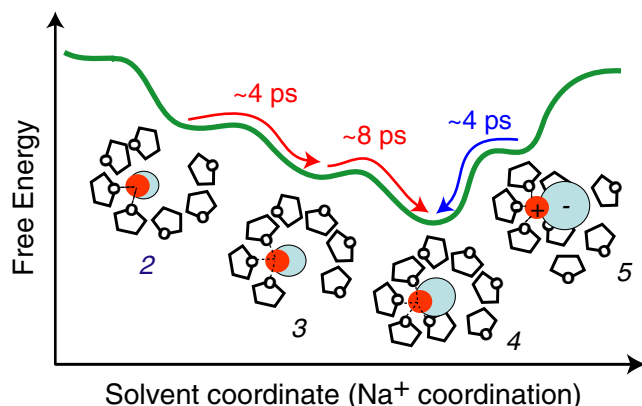
FIG. 3 (color online). Schematic free-energy surface illustrating the solvation coordinate of the neutral sodium TCP in liquid THF. The solvation coordinate is characterized by the number of THF molecules coordinated to Na^+ (red circle, +) via their oxygen sites. Dynamic solvation involves discrete steps between different coordination motifs and degrees of electron (blue oval, −) displacement from Na^+. The free-energy surface is drawn to emphasize that these solvent-solute motifs are chemically distinct species (albeit transiently lived) and that the relaxation of this solvent-solute system progresses through a specific sequence of solvation structures to reach equilibrium.

carry the system between solvent-solute configurations at equilibrium. To bolster this idea, the solid and dashed curves in Fig. 2(c) show the time dependence of the spectral features in Fig. 2(b), while the orange dotted curve shows the temporal response of TCP solvation at 1130 nm measured in a separate experiment [2]. Clearly, Figs. 2(b) and 2(c) reveal that nonequilibrium solvation occurs through a specific sequence of solvent-solute configurations, as illustrated schematically in the left half of Fig. 3. Thus, we have directly observed the discrete rearrangement of local solvent molecules coordinating the cation end of the TCP during relaxation along a nonequilibrium solvation coordinate in a room-temperature liquid.

In previous work, we compared the nonequilibrium relaxation of the neutral sodium TCP prepared following photodetachment from Na^- to that following photoinduced electron attachment to Na^+ [10]. We found that the rate of the solvent relaxation that brings the TCP to equilibrium along these two pathways differed by a factor of 2, which we interpreted as a breakdown of the linear response approximation [1,10]. The data in Figs. 1 and 2 allow us to interpret why this breakdown occurs: The relaxation of the TCP following photodetachment of electrons from Na^- occurs via the same solvent fluctuations that convert the twofold- and threefold-coordinated motifs into the fourfold-coordinated configuration that dominates at equilibrium. In contrast, when TCPs are created via photoinduced electron attachment to Na^+, the nascent nonequilibrated configuration is overcoordinated because Na^+ is coordinated by six THF molecules prior to the arrival of the electron. This is consistent with our observation that the spectrum of the nonequilibrium (Na^+, e^-)

TCPs created via photoinduced attachment is redshifted before relaxing to equilibrium [10]. Thus, nonequilibrium solvation in this case is dominated by the $5 \rightarrow 4$ conversion, so that this solvation time scale reflects the motion of a single solvent molecule losing its coordination to the cation end of the TCP (right half of Fig. 3).

Figure 3 summarizes the fact that a greater number of molecular steps are required to solvate an ensemble of initially undercoordinated TCP solute-solvent configurations (prepared via photodetachment from Na^- or THB) than initially overcoordinated configurations (prepared via photoattachment to Na^+), so that it takes longer for initially undercoordinated TCPs to reach the dominant solvent-solute configuration present at equilibrium. Thus, the difference in spectral dynamics and solvation time scales along these two relaxation pathways directly reflects a specific asymmetry in the solvation coordinate for this simple system. Importantly, the molecular-level picture we derive from the data in Figs. 1 and 2 underscores how solvent relaxation is intimately tied to the specific molecular rearrangement of solvent molecules accompanying a given nonequilibrium perturbation. Moreover, the sequential, single-molecule nature of the relaxation indicates that a continuum description of solvation is inappropriate.

*Current Address: Department of Chemistry, Stanford University, Stanford, CA 94305, USA.
†To whom correspondence should be addressed. schwartz@chem.ucla.edu.

[1] R. M. Stratt and M. Maroncelli, J. Phys. Chem. **100,** 12 981 (1996).
[2] M. C. Cavanagh, R. E. Larsen, and B. J. Schwartz, J. Phys. Chem. A **111,** 5144 (2007).
[3] R. Catterall, J. Slater, and M. C. R. Symons, J. Chem. Phys. **52,** 1003 (1970).
[4] B. Bockrath and L. M. Dorfman, J. Phys. Chem. **77,** 1002 (1973).
[5] F.-Y. Jou and G. R. Freeman, Can. J. Chem. **57,** 591 (1979).
[6] W. J. Glover, R. E. Larsen, and B. J. Schwartz (to be published).
[7] See supplementary material at http://link.aps.org/supplemental/10.1103/PhysRevLett.104.233005 for a PDF file that contains additional details.
[8] G. R. Fleming, *Chemical Applications of Ultrafast Spectroscopy* (Oxford University Press, New York, 1986).
[9] A. E. Bragg and B. J. Schwartz, J. Phys. Chem. A **112,** 3530 (2008).
[10] A. E. Bragg, M. C. Cavanagh, and B. J. Schwartz, Science **321,** 1817 (2008).
[11] O. Shoshana, J. L. Pérez Lustres, N. P. Ernsting, and S. Ruhman, Phys. Chem. Chem. Phys. **8,** 2599 (2006).